DOI: https://doi.org/10.24425/amm.2026.1983

ŁUKASZ MAJOR[1*], JÜRGEN M. LACKNER[2], DIETMAR KOPP[2], BOGUSŁAW MAJOR[1]

SELF-LUBRICATING AND SELF-HEALING MoS_2/WS_2 NANOCOATINGS ON POLYMERS DEPOSITED BY APPJ: A COMPREHENSIVE REVIEW

High-performance polymers (PEEK, PA11) are vital in lightweight engineering but limited by friction and wear. This review analyzes self-lubricating and self-healing MoS_2 and WS_2 coatings deposited via atmospheric pressure plasma jet (APPJ). By integrating recent literature with the authors' previous studies [25,26], the paper evaluates coating design, microstructure, and tribology on polymer substrates. While lamellar sliding ensures low friction, WS_2 offers stability in humidity, and MoS_2 provides adaptive self-healing via crack filling. The review concludes that optimized coatings significantly enhance durability and provide guidelines for designing high-performance, multifunctional polymer surfaces.

Keywords: MoS_2 and WS_2 nanocoatings; polymer substrates; atmospheric pressure plasma jet (APPJ); wear and self-lubrication; nanoscale tribology

1. Intruduction

High-performance polymers, including polyether ether ketone (PEEK) and polyamide 11 (PA11), are increasingly employed in advanced engineering applications requiring lightweight, chemical stability, and mechanical robustness [1-4]. Despite their favorable bulk properties, these materials exhibit relatively high coefficients of friction and limited wear resistance under dry sliding conditions, restricting their use in tribologically demanding environments [5-12]. Improving the surface performance of polymeric components while understanding the underlying nanoscale mechanisms of wear and degradation remains a critical challenge in materials science.

A common strategy to enhance tribological performance involves the deposition of lamellar solid lubricants, such as molybdenum disulfide (MoS_2), tungsten disulfide (WS_2), and graphite, often combined with metal binders like zinc (Zn) [13-16]. MoS_2 is widely recognized for its excellent lubricity and interlayer sliding mechanism, which facilitates low friction and self-lubricating behavior [17-22]. However, MoS_2 is sensitive to moisture and oxidative conditions, potentially leading to MoO_3 formation and deteriorated performance [23]. In contrast, WS_2 exhibits higher thermal and oxidative stability, maintaining effective low-friction behavior even in humid environments, making it a promising alternative for next-generation coatings [13,24]. Composite coatings combining MoS_2 or WS_2 with metals and carbon-based additives have demonstrated enhanced wear resistance and the potential for self-healing through micro-crack closure and the reconstruction of van der Waals bonds [13,19]. While conventional vacuum-based techniques, such as sputtering, produce high-quality coatings, they often face limitations on polymer substrates due to high process temperatures and adhesion issues.

Low-temperature atmospheric pressure plasma deposition (APPD), specifically utilizing atmospheric pressure plasma jets (APPJ), has emerged as a scalable and energy-efficient alternative. This approach enables the deposition of functional nanocoatings on temperature-sensitive polymers without vacuum systems, allowing precise control over surface chemistry. APPJ-mediated deposition has been shown to produce MoS_2- and WS_2- based coatings with excellent adhesion, low friction, and self-healing capabilities [25, 26].

Despite these advances, a systematic comparison of MoS_2- and WS_2- based coatings on polymer substrates, focused on nanoscale mechanisms and the role of metal binders, remains limited. This review aims to synthesize recent developments

1 INSTITUTE OF METALLURGY AND MATERIALS SCIENCE, POLISH ACADEMY OF SCIENCES, 25 REYMONTA STR., 30-059 KRAKÓW, POLAND
2 JOANNEUM RESEARCH FORSCHUNGSGESELLSCHAFT MBH, INSTITUTE FOR SENSORS, PHOTONICS AND MANUFACTURING TECHNOLOGIES, RESEARCH GROUP LASER AND PLASMA PROCESSING, LEOBNER STRASSE 94, 8712 NIKLASDORF, AUSTRIA

* Corresponding author:

in APPJ-deposited nanocoatings, highlighting their tribological performance and self-healing mechanisms to provide insights for future engineering of polymer-supported lubricating films.

2. Materials and methods

2.1. Specimen preparation

The polymer substrates discussed in this review were based on previously reported studies [25,26] involving unfilled polyether ether ketone (PEEK, TECAPEEK MT natural, Ensinger®, Austria) and polyamide 11 (PA11). In those investigations, PEEK rods were sectioned into disks with a thickness of 5 mm. The surface preparation involved sequential wet grinding using SiC abrasive papers (grit #500 and #1000) to ensure uniform surface roughness. Subsequently, the specimens underwent ultrasonic cleaning in 2-propanol (≥99.5%) for 10 min and were thoroughly dried before coating deposition. PA11 substrates were prepared using the same polishing and cleaning procedures to ensure comparable surface conditions across all tested systems.

2.2. Coatings deposition

The coatings analyzed in this review were fabricated in two distinct experimental series using the same atmospheric pressure plasma jet (APPJ) technique [25,26]. The first system comprised WS_2/Zn coatings deposited on PEEK substrates. The feedstock powder, consisting of 75 wt.% WS_2 (Tribotecc® GmbH, Austria) and 25 wt.% Zn (ECKART®, Germany), was homogenized in a TURBULA® 3D mixer for 30 min. Particle size distribution was verified by laser diffraction after dispersion in ethanol (≥96%). The fine powder fraction (<10 μm) was delivered to the APPJ system via a brush feeder (TwinoFeed, INO®, Austria). Deposition was performed using optimized parameters: a plasma jet current of 100 A, a nozzle-to-substrate distance of 30 mm, and a scanning velocity of 200 mm/s over five linear passes. Argon served as the carrier gas (10-20 L/min), with nitrogen shrouding applied in specific variants to control the atmosphere. The second system involved MoS_2/graphite/Zn coatings deposited on PA11 substrates, utilizing the same APPJ-based deposition approach to ensure methodological consistency. The feedstock was composed of 50 wt.% MoS_2 (OKS 100, purity >97.7%), 25 wt.% graphite (MOS C80, Tribotecc®, purity >87.8%), and 25 wt.% Zn (ECKART®, purity >95.6%). This mixture was homogenized in a TURBULA® mixer for 15 min. The formulation (designated as V4 in previous studies) was optimized to enhance interfacial adhesion between the PA11 substrate and the composite lubricating matrix. This configuration was specifically designed to promote low-friction behavior and adaptive tribological responses, including the self-healing mechanisms further discussed in this review.

2.3. Microstructural characterization

Microstructural analyses summarized in this review were conducted using scanning electron microscopy (SEM) and transmission electron microscopy (TEM) data from the original investigations [25,26]. SEM observations were performed on a Scios 2 DualBeam (Thermo Fisher Scientific) microscope, employing both high-voltage bulk imaging and low-voltage surface analysis to minimize interaction volume. High-resolution imaging of surface topography and phase contrast was achieved using in-lens Trinity detectors for secondary and backscattered electrons. For cross-sectional nanoscale analysis, site-specific TEM lamellae were extracted via focused ion beam (FIB) milling using SCIOS 2 DualBeam microscope (Galium ion column) and AutoTEM 4 software. Subsequent TEM investigations were carried out on a Themis (Thermo Fisher Scientific) microscope equipped with field emission gun (FEG), operating at 200 kV in bright-field (BF), high-resolution (HRTEM), and scanning/transmission (STEM) modes. Phase identification was performed using selected area electron diffraction (SAED), while elemental distribution and chemical composition were mapped via energy-dispersive X-ray spectroscopy (EDS). These advanced characterization techniques provided critical insights into the lamellar architecture, interfacial bonding, and nanoscale structural evolution of the WS_2/Zn and MoS_2/graphite/Zn systems.

2.4. Tribological testing

Tribological performance data summarized in this review originate from ball-on-disk experiments conducted using a TRB^3 tribometer (Anton Paar®) in rotational mode [25,26]. Hardened 100Cr6 steel balls (diameter: 6 mm; hardness: 60-62 HRC) served as counterbodies and were ultrasonically cleaned in ethanol (≥96%) prior to each test. For the WS_2/Zn coatings on PEEK, tests were performed at two wear-track diameters (10 mm and 20 mm) at a constant linear velocity of 25 mm/s under a normal load of 1 N. This load corresponded to an initial maximum Hertzian contact stress of approximately 79 MPa for the PEEK-steel contact. Sliding distances ranged from 100 m to 628 m, depending on the specific track diameter and experimental objectives. The MoS_2/graphite/Zn coatings on PA11 were evaluated under analogous kinematic conditions to facilitate a comparative assessment of frictional behavior and adaptive tribological responses, including the previously reported self-healing effects. To ensure statistical reliability, all measurements were performed in triplicate. The specific wear rate (k) was calculated using the following expression:

$$k = \frac{V}{F * s}$$

where V represents the wear volume (mm^3), F is the normal load (N), and s is the total sliding distance (m). Furthermore, long-term sliding tests from the source studies were analyzed to evaluate the stability and durability of the formed tribofilms under extended operational cycles.

3. Results and discussion: Comparative Analysis of MoS_2- and WS_2- Based Nanocoatings

The tribological performance of nanostructured coatings on polymer substrates is fundamentally dictated by the interplay between chemical composition and microstructural architecture.

3.1. WS_2/Zn systems on PEEK

WS_2/Zn coatings deposited on PEEK by gas-shrouded atmospheric pressure plasma jet (APPJ) demonstrated a pronounced sensitivity of the coefficient of friction (COF) to deposition parameters. The lowest and most stable COF (0.18±0.02) was achieved with a 15 L/min powder flow rate (sample E4), whereas higher flow rates led to increased friction and accelerated wear [13,26] (Fig. 1).

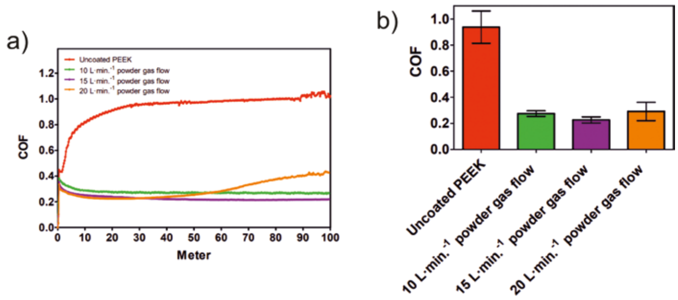

Fig. 1. Tribological properties of WS_2-Zn coatings deposited on PEEK at 100 A: a) plasma current versus powder gas flow rate over a 100 m sliding distance; b) corresponding average friction coefficient (COF) values [13,26]

This trend correlates directly with microstructural evolution: at 15 L/min, an optimized lamellar WS_2 network was effectively embedded within the Zn matrix (Figs. 2 and 3), promoting interplanar sliding and the formation of a continuous tribofilm (Figs. 4-6).

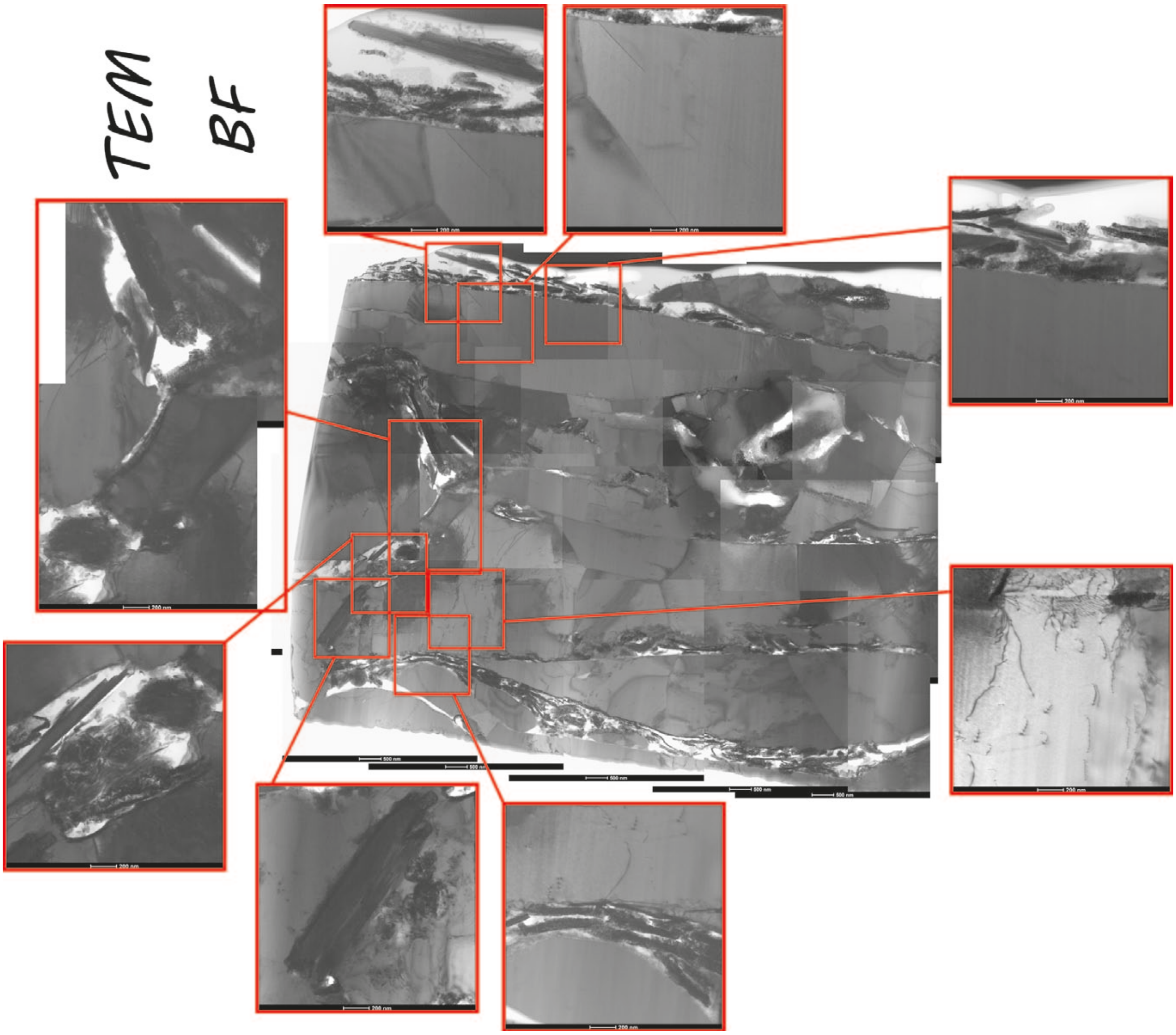

Fig. 2. TEM bright-field (BF) micrograph of the coating cross-section deposited at a powder gas flow rate of 15 L/min [26]

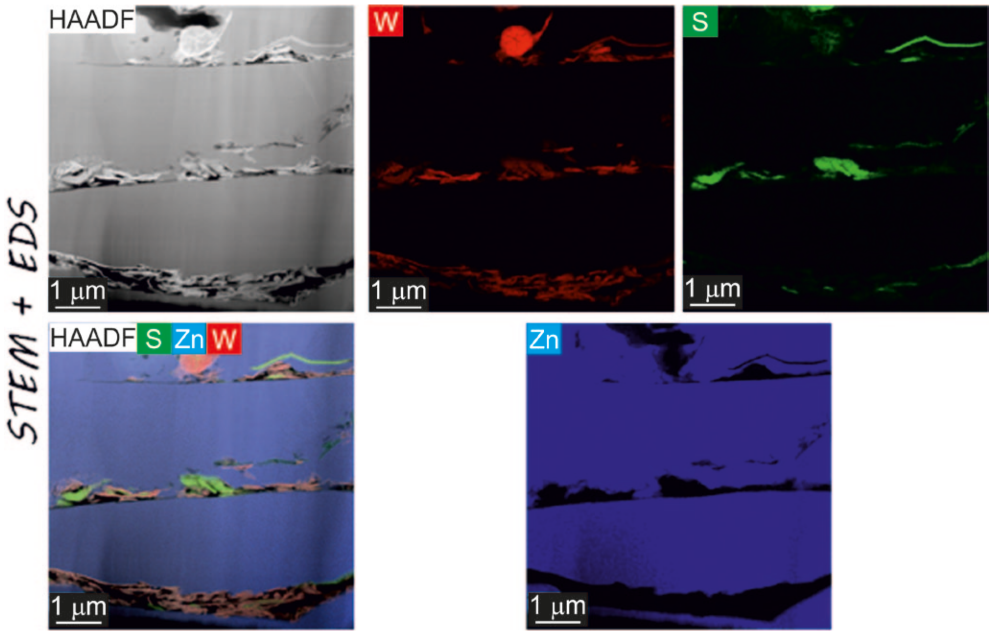

Fig. 3. Qualitative EDS elemental mapping showing the chemical composition distribution for the coating produced at 15 L/min powder gas flow [26]

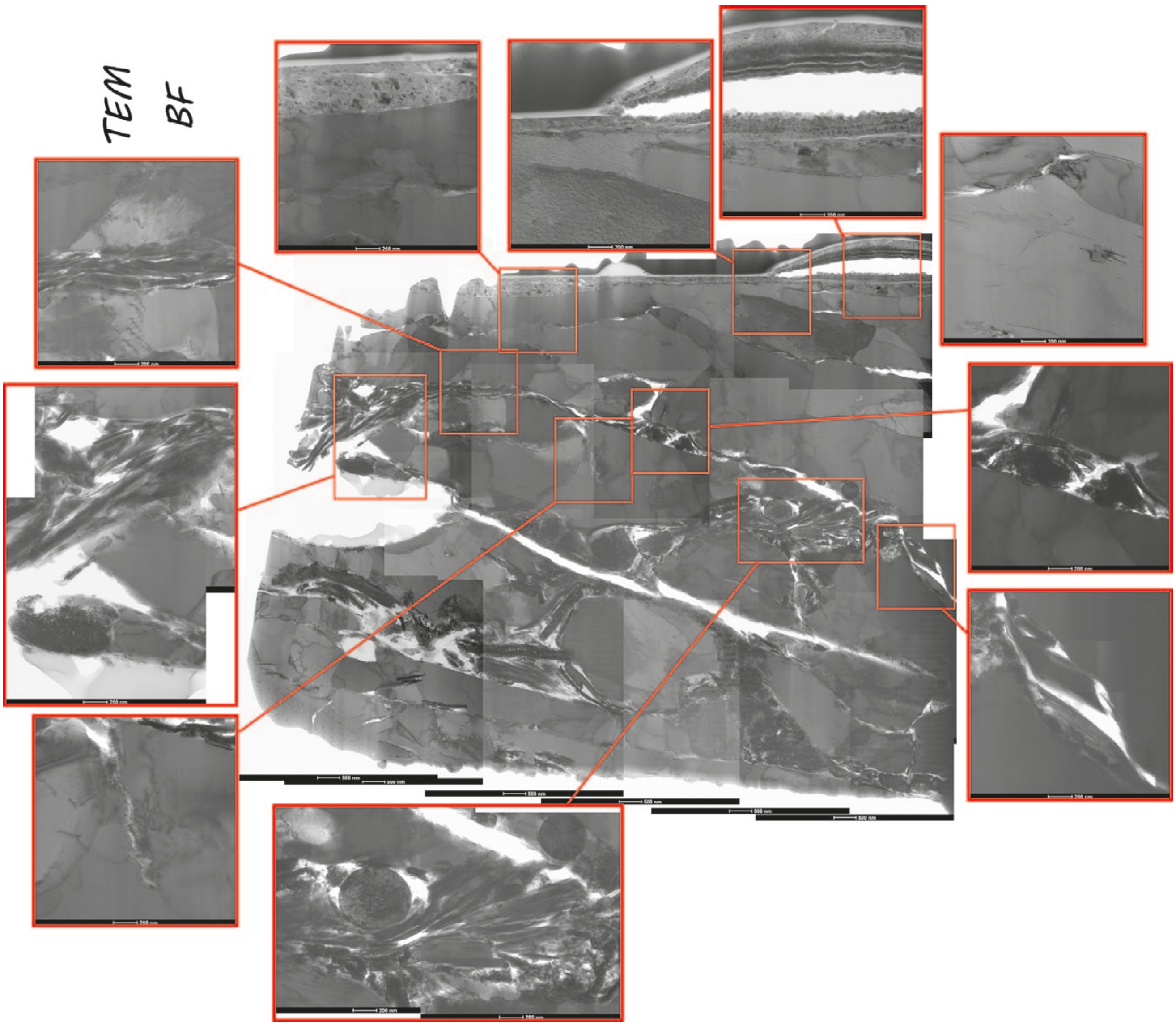

Fig. 4. Post-tribological TEM BF cross-sectional characterization of the coating deposited at 15 L/min powder gas flow [26]

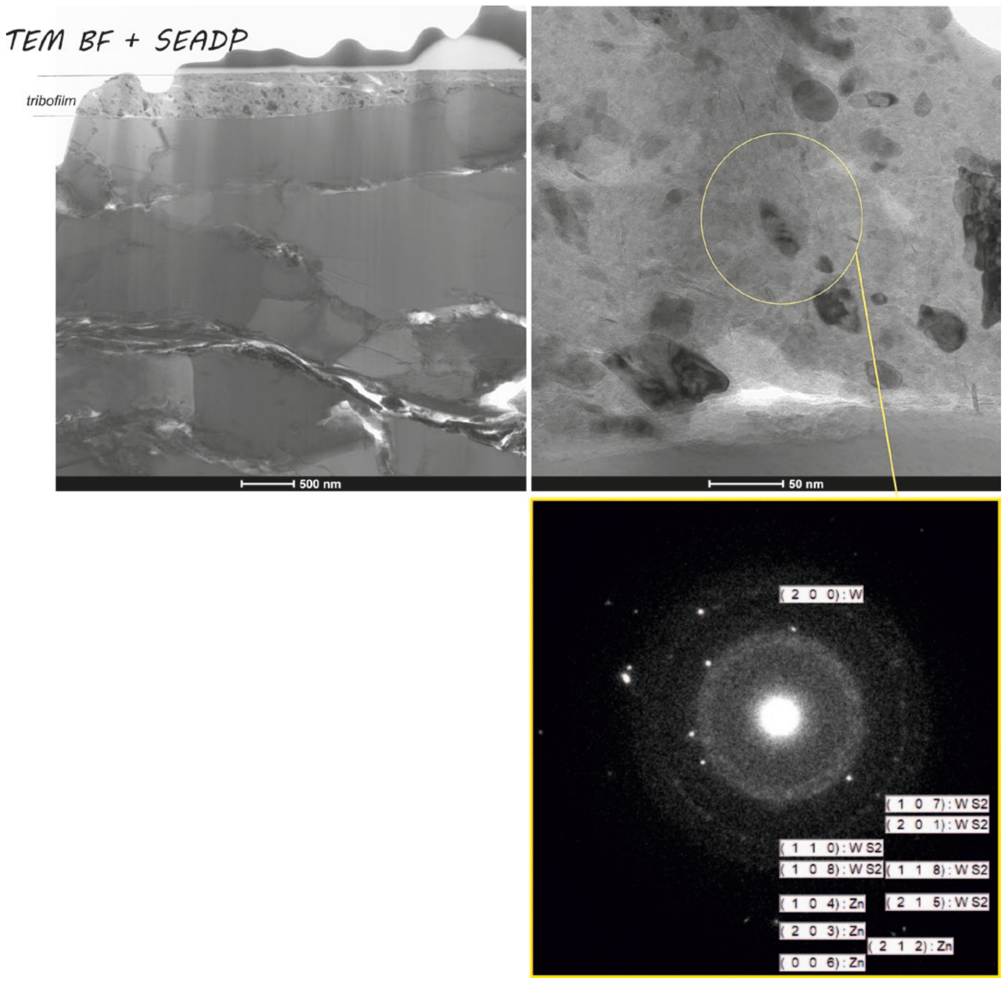

Fig. 5. TEM BF analysis of the tribofilm developed during wear testing (15 L/min powder gas flow): a) TEM BF image; b) phase identification via selected area electron diffraction pattern (SAEDP) [26]

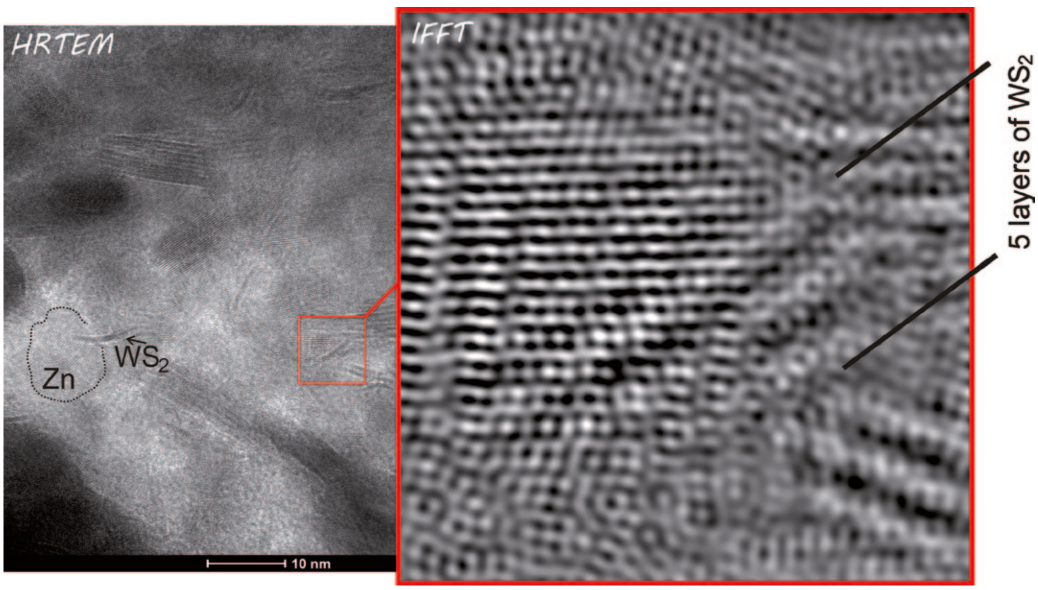

Fig. 6. High-resolution TEM (HRTEM) micrograph of the tribofilm formed on the coating deposited at 15 L/min powder gas flow [26]

Conversely, insufficient WS_2 incorporation at higher flow rates (Figs. 7 and 8) resulted in fragmented lamellae, compromising both frictional stability and tribofilm integrity (Figs. 9-11). To provide a deeper insight into the wear mechanism, the degradation of these coatings primarily involves abrasive wear combined with micro-ploughing of the Zn matrix during the

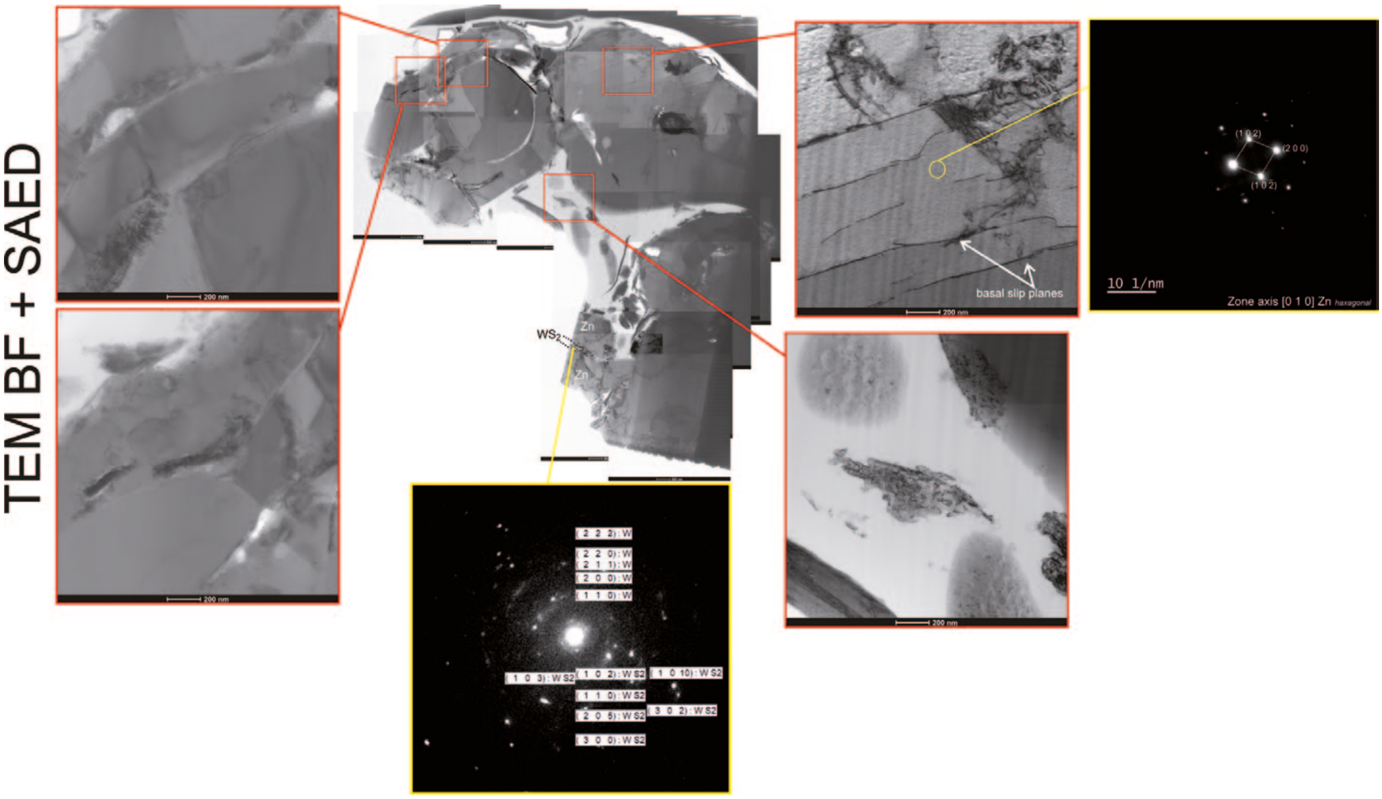

Fig. 7. Cross-sectional TEM BF image of the as-deposited coating produced at a 20 L/min powder gas flow rate [26]

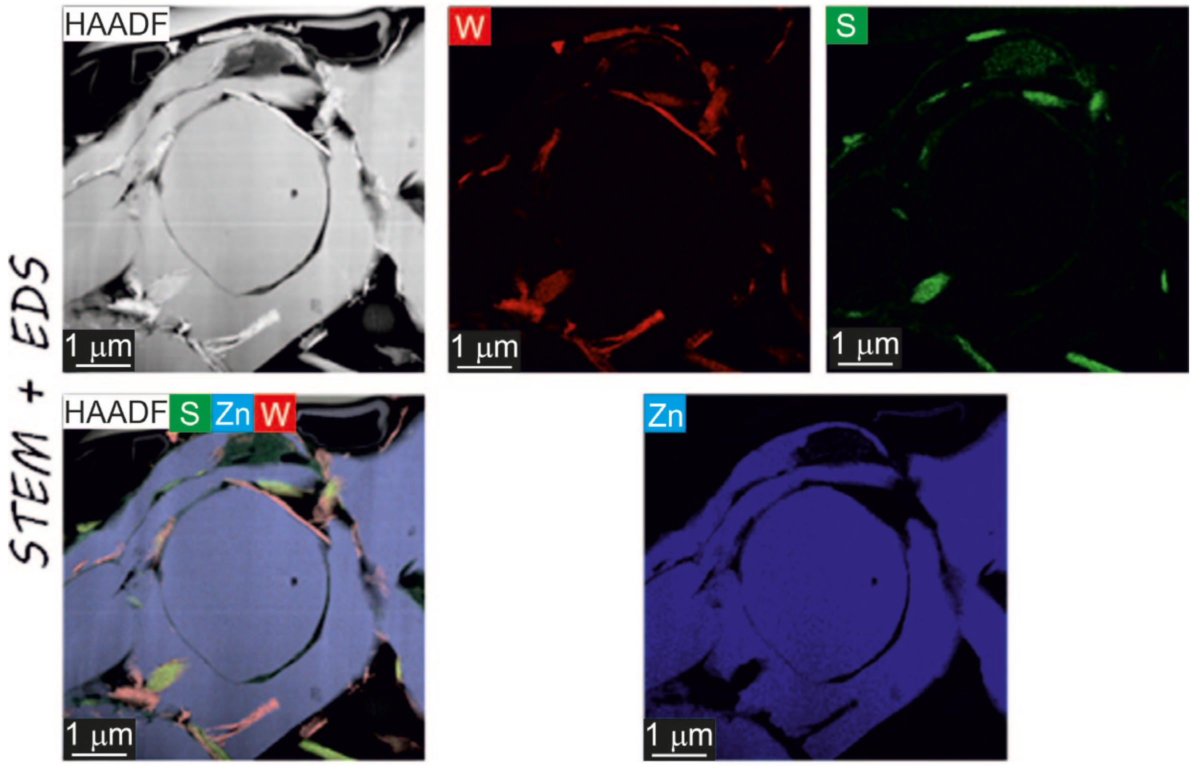

Fig. 8. EDS chemical maps illustrating the distribution of key elements in the as-deposited coating (20 L/min powder gas flow) [26]

initial sliding stages. The continuous shearing of the optimized lamellar network facilitates the exfoliation of WS_2 basal planes. This process leads to the progressive coverage of the contact zone, effectively preventing direct metal-to-polymer contact. In contrast, when the lamellae are fragmented due to improper flow rates, the localized stress concentration accelerates coating delamination and debris generation, which destabilizes the tribofilm.

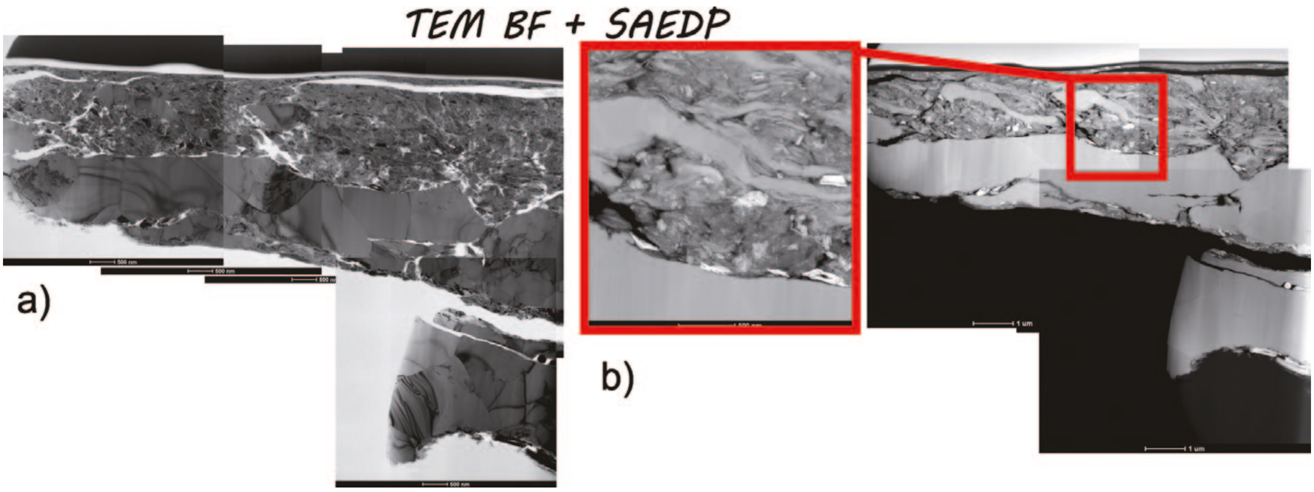

Fig. 9. Microstructural examination of the wear-tested coating (20 L/min powder gas flow): a) TEM BF image; b) STEM image of the cross-section [26]

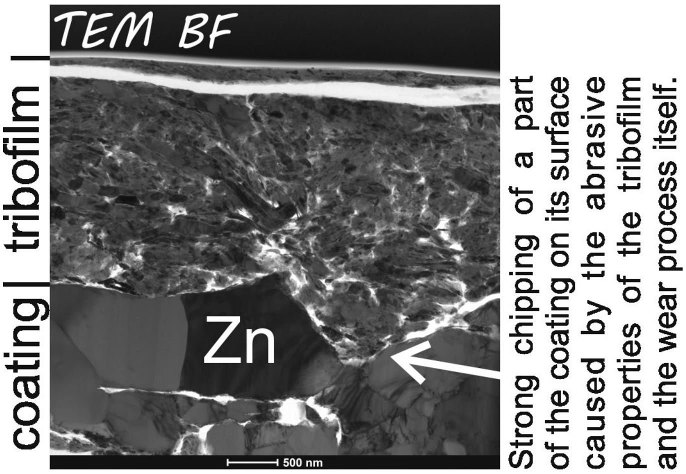

Fig. 10. TEM BF characterization of the interface between the coating and the tribofilm (20 L/min flow rate), highlighting the detrimental effect of this layer on wear resistance [26]

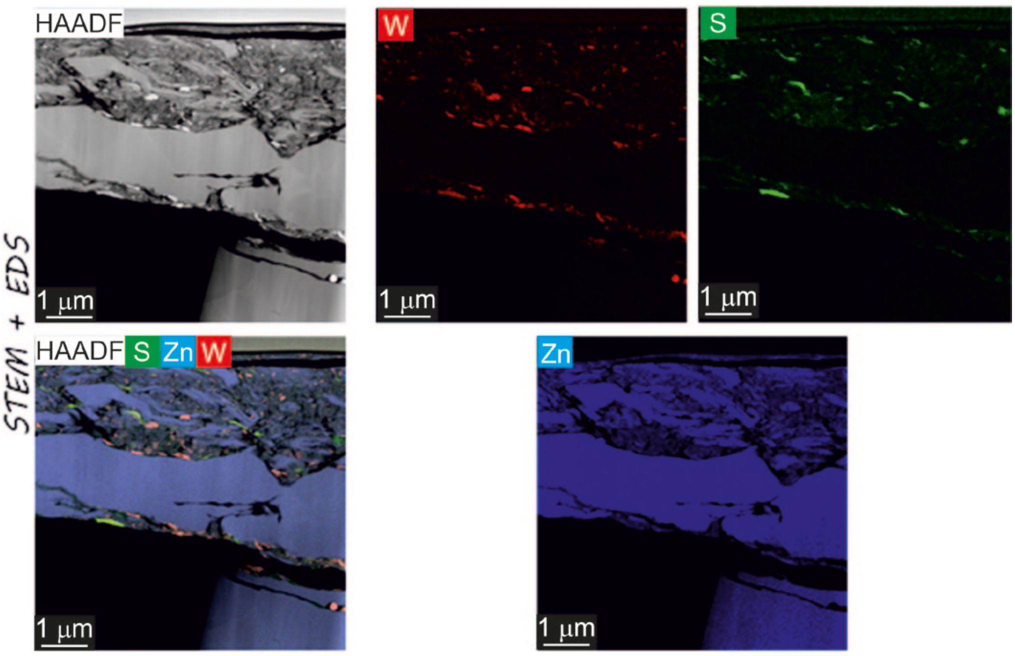

Fig. 11. Elemental EDS analysis of the tribofilm generated during the wear process for the 20 L/min gas flow variant [26]

3.2. MoS_2/graphite/Zn systems on PA11

In contrast, MoS_2/graphite/Zn coatings on PA11, produced via the same APPJ-based deposition technique, exhibited multi-functional self-lubricating and self-healing behavior [25].

Cross-sectional SEM and TEM analyses revealed a complex composite microstructure where MoS_2 and graphite layers alternated with Zn-rich regions (Figs. 12-14).

Deformation mechanisms in MoS_2 and graphite included kinking and interlayer sliding and delamination via van der Waals bond cleavage, forming multi-layered lubricating bands. Under mechanical load, micro-cracks within the Zn matrix (Fig. 15) were progressively filled by the migration of MoS_2 and graphite, creating self-healing lamellar structures that maintained low friction throughout the sliding process (Figs. 16 and 17). The self-healing functionality in these systems is driven by a combination

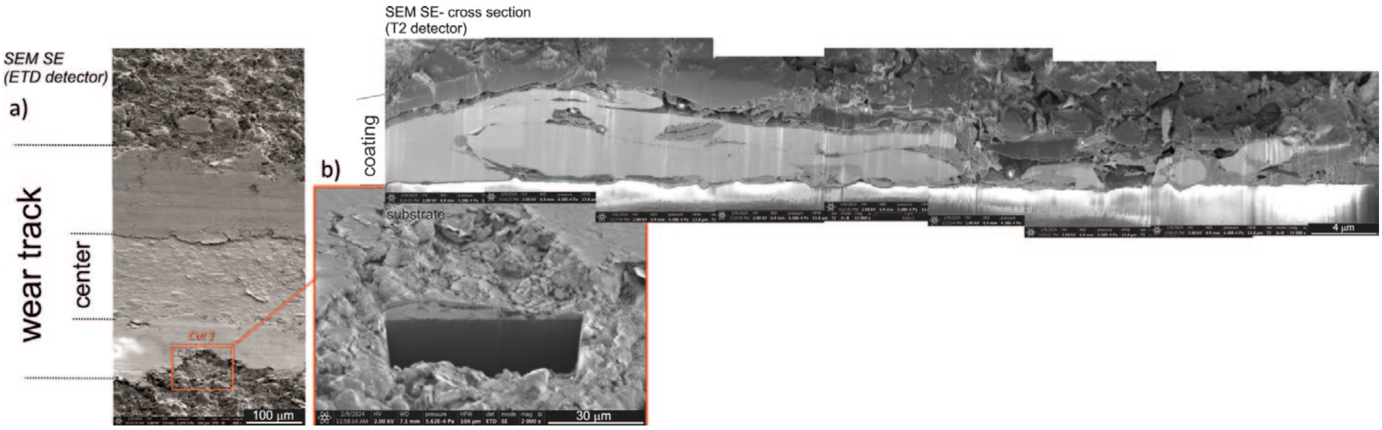

Fig. 12. SEM (SE) topographic images of the wear track: a) plan view; b) cross-sectional view indicating the area selected for subsequent TEM analysis [25]

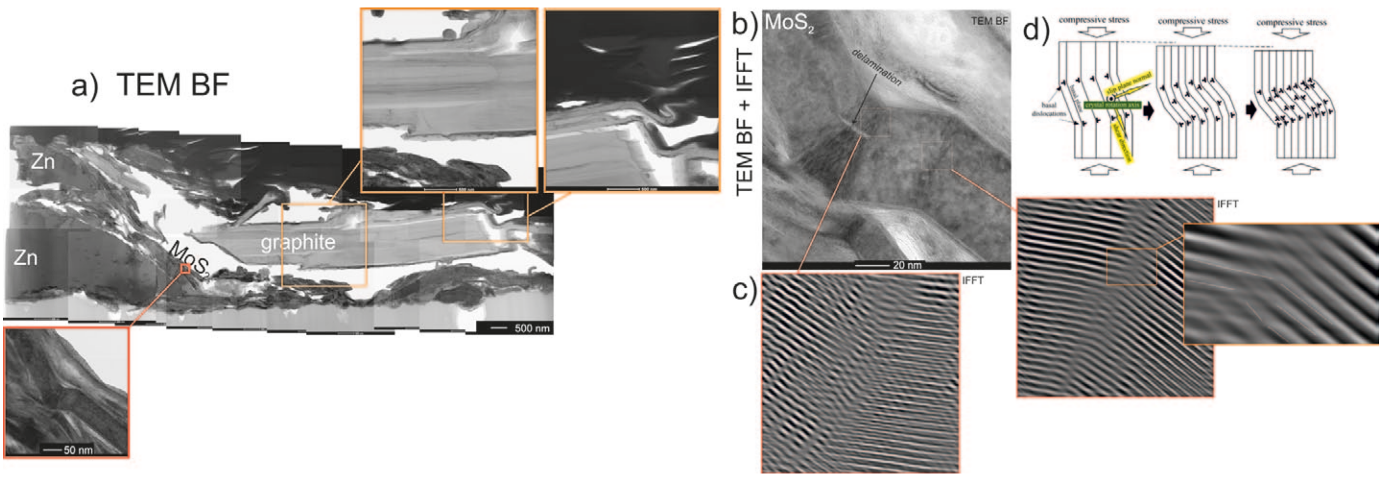

Fig. 13. Comprehensive cross-sectional analysis near the wear track: a) TEM BF image; b) visualization of the kinking deformation mechanism; c) IFFT image; d) schematic representation of the kinking process [25]

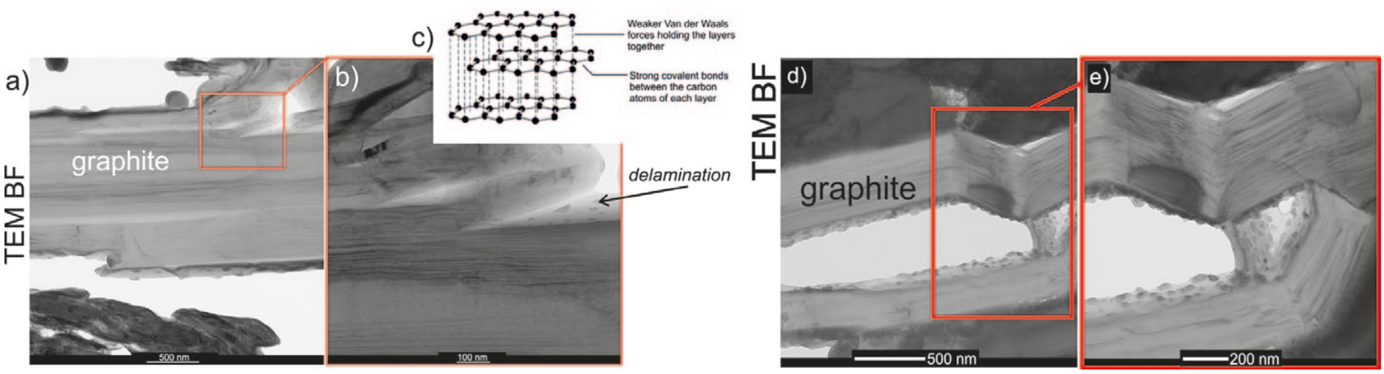

Fig. 14. Investigation of the wear mechanism within the graphite phase: a) TEM BF image; b) magnification of the kinking effect; c) schematic of the graphite atomic layer arrangement [25]

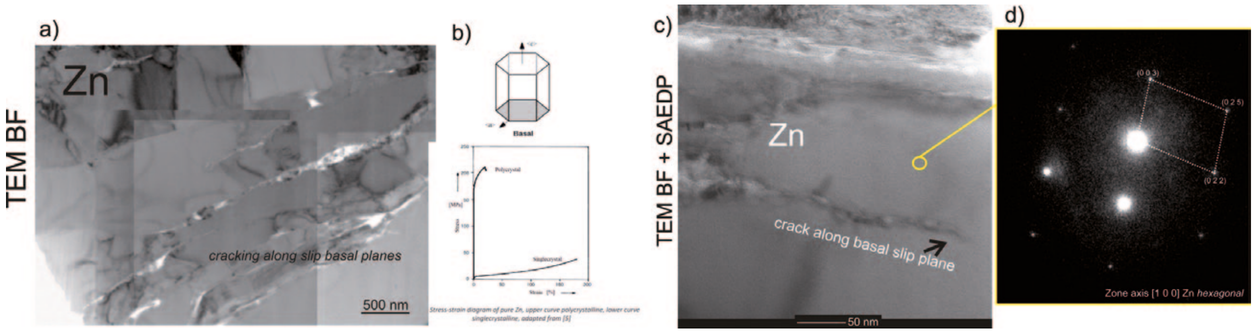

Fig. 15. Investigation of the wear mechanism within the graphite phase: a) TEM BF image; b) magnification of the kinking effect; c) schematic of the graphite atomic layer arrangement [25]

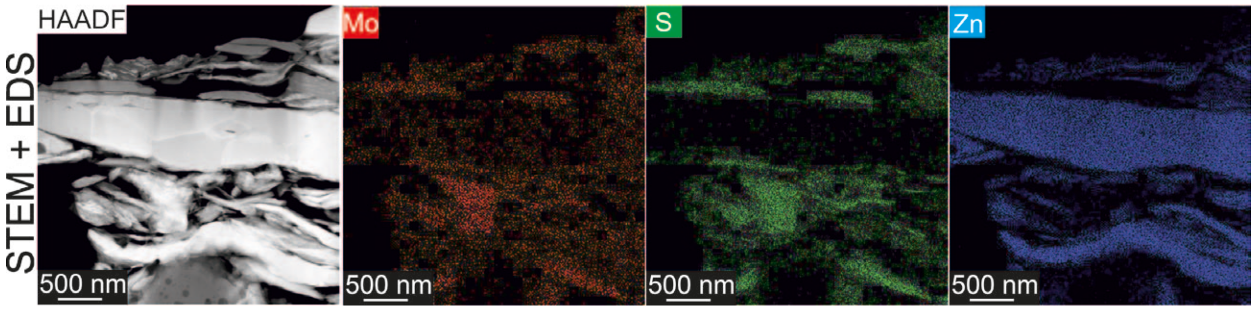

Fig. 16. Combined STEM and EDS qualitative chemical mapping of the coating cross-section [25]

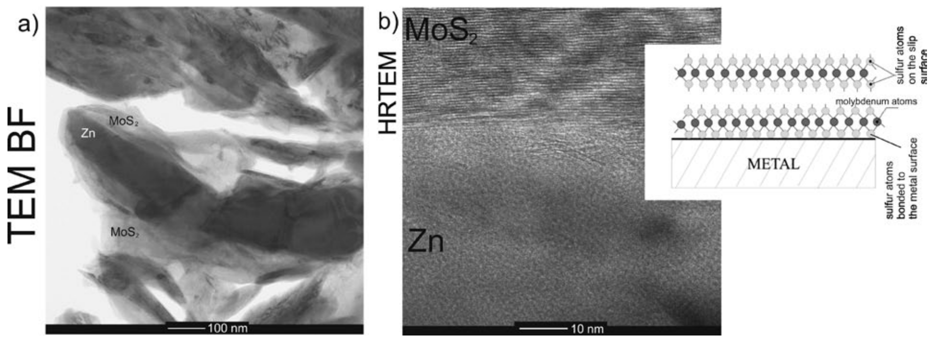

Fig. 17. Microstructural evidence of the self-healing effect: a) TEM BF image; b) HRTEM image with a schematic model of the MoS_2 atomic layer arrangement [25]

of mechanical triggering and material migration. Under localized stress, the kinking and delamination of MoS_2 and graphite layers lower the shear strength within the composite. This allows the solid lubricants to plastically deform and flow into the micro-cracks formed in the Zn matrix. This stress-induced migration mechanically seals the defects, preventing crack propagation and restoring the structural integrity of the lubricating layer, which ensures sustained low friction.

3.3. Comparative synthesis

A direct comparison highlights fundamental mechanistic differences. WS_2 coatings achieve low friction primarily through stable lamellar sliding and robust tribofilm coverage, with performance strictly dependent on precise powder flux control. MoS_2- based coatings, while also utilizing lamellar sliding, offer active self-healing facilitated by the dynamic filling of micro-cracks and potential chemisorption of sulfur to the Zn binder [25,27]. However, environmental sensitivity remains a distinguishing factor: MoS_2 is more susceptible to moisture-induced degradation, whereas WS_2 maintains more consistent performance in humid conditions [24,28]. Ultimately, while WS_2 offers superior environmental stability and reproducibility, MoS_2 provides adaptive self-repair mechanisms that may extend the operational lifetime of polymer components under cyclic loading.

4. Design considerations and practical implications

The comparative analysis of WS_2- and MoS_2- based nanocoatings highlights several critical factors for designing durable, high-performance lubricating films on polymers.

4.1. Material synergy and microstructural control

Both systems rely on metallic binders, such as Zn, to enhance structural integrity. In WS_2/Zn coatings, Zn provides a stiff matrix that supports the lamellar network, which is essential for stable tribofilm formation [26]. In MoS_2/graphite/Zn coatings, the Zn matrix facilitates self-healing by acting as a host for lubricant migration into micro-cracks [25]. Furthermore, the inclusion of graphite complements MoS_2 by providing additional van der Waals-mediated sliding layers, enhancing performance under cyclic loading.

4.2. Environmental and operational selection

Material selection must be driven by the operating environment. WS_2 is preferred for applications exposed to variable humidity due to its superior oxidative stability [24]. Conversely, MoS_2- based systems are ideal for dry, high-load conditions where their active self-healing mechanisms can counteract localized surface damage.

4.3. Future directions

To advance polymer-supported nanocoatings, future research should focus on:

– Hybrid Systems: Combining WS_2 and MoS_2 to merge environmental robustness with adaptive self-healing.
– Modeling: Developing quantitative models for lamellar deformation and tribofilm evolution.
– Sustainability: Ensuring scalable, vacuum-free deposition remains energy-efficient and environmentally benign.

5. Conclusions

This review demonstrates that atmospheric pressure plasma jet (APPJ) deposition is a highly versatile and effective method for engineering multifunctional nanocoatings on high-performance polymers. The low-temperature nature of the process allows for the successful integration of MoS_2 and WS_2 solid lubricants onto temperature-sensitive substrates like PEEK and PA11 without compromising their bulk properties. Comparative analysis reveals that while both systems significantly enhance tribological performance, their effectiveness is governed by distinct nanoscale mechanisms. For WS_2/Zn coatings, structural integrity and low friction are strictly tied to the precision of deposition parameters, which dictate the formation of a stable lamellar network. In contrast, the MoS_2/graphite/Zn system introduces an active, adaptive dimension through self-healing; the stress-induced migration of lubricant phases into micro-cracks effectively extends the operational lifetime of the coating under cyclic loading.

Ultimately, the choice between these two systems involves a strategic trade-off between environmental stability and adaptive resilience. While WS_2 offers more consistent performance in humid conditions, MoS_2 provides superior self-repair capabilities in dry environments.

These findings provide a clear framework for the design of next-generation, polymer-supported lubricating films, suggesting that future developments should focus on hybridizing these lubricants to combine environmental robustness with active self-healing functionality.

Acknowledgements

This work was financially supported by the: Projects “functionalWOOD-2print”, “ThermoMelt4PA” and “sustainableSLS” funded by Austrian Research Promotion Agency (FFG), by the Federal Ministry of Agriculture, Forestry, Regions and Water Management, through their funding program “Think.Wood” of the Austrian Wood Initiative as well as within the statutory work in the Institute of Metallurgy and Materials Science PAS- Z-14/2026

REFERENCES

[1] P.D. Neis, N.F. Ferreira, J.C. Poletto, J. Sukumaran, M. Andó, Y. Zhang, Tribological behavior of polyamide-6 plastics and their potential use in industrial applications. Wear **376-377**, 1391-1398 (2017).
DOI: https://doi.org/10.1016/j.wear.2017.01.090

[2] S.F.A. Abdullah, S.S. Md Saleh, N.F. Mohammad, S.N. Syed Mahamud, M.F. Omar, H.Md Akil, B.P. Chang, H.R. Saliu, N.H. Rostam, J. Gondro, Effect of Nitrate Acid Treated Dolomite on the Tensile Properties of Ultra-High Molecular Weight Polyethylene (UHMWPE) Composites. Arch. Metall. Mater. **69**, 281-288 (2024).
DOI: https://doi.org/10.24425/amm.2024.147820

[3] F. Song, Q. Wang, T. Wang, The effects of crystallinity on the mechanical properties and the limiting PV (pressure velocity) value of PTFE. Tribol. Int. **93**, 1-10 (2015).
DOI: https://doi.org/10.1016/j.triboint.2015.09.017

[4] M.A. Platon, O. Nemeș, A.-E. Tiuc, C. Vilău, C.M. Dudescu, S. Pădurețu, The Influence of Process Parameters on the Mechanical Behavior of a Composite Material Made from Mixed Plastic Wastes. Arch. Metall. Mater. **67**, 1235-1241 (2022).
DOI: https://doi.org/10.24425/amm.2022.141047

[5] M. Andó, J. Sukumaran, V. Rodrigez, P. Neis, G. Kalácska, T. Czigány, P. De Baets, Development of new PA6 composites. Mech. Eng. Lett.: Res. Dev. **5** (5), 145-154 (2011).

[6] E. Abele, G. Reinhart, Zukunft der Produktion. Carl Hanser Verlag GmbH & Co, München (2011).

[7] B. Wendel, D. Rietzel, F. Kühnlein, R. Feulner, G. Hülder, E. Schmachtenberg, Additive processing of polymers. Macromol. Mater. Eng. **293** (10), 799-809 (2008).
DOI: https://doi.org/10.1002/mame.200800121

[8] A. Gebhardt, Generative Fertigungsverfahren- Additive Manufacturing und 3D Drucken für Prototyping – Tooling – Produktion. Carl Hanser Verlag, München (2013).

[9] T. Oswald, E. Bauer, S. Brinkmann, K. Oberbach, E. Schmachtenberg, International Plastics Handbook. 30th Edition, Carl Hanser Verlag, München (2006).

[10] S. Yu, C. Zhu, H. Wu, L. Yao, M. Mahapatra, Y. Xu, Graphite-enhanced PTFE/PEEK composite coating for improved friction and wear resistance. Appl. Surf. Sci. 7**00**, 163214 (2025). DOI: https://doi.org/10.1016/j.apsusc.2025.163214

[11] K. Banerjee, M. Debroy, V.K. Balla, S. Bodhak, Recent progress in 3D-printed polyaryletherketone (PAEK)-based high-performance polymeric implants for musculoskeletal reconstructions. J. Mater. Res. **36**, 3877-3893 (2021). DOI: https://doi.org/10.1557/s43578-021-00231-4

[12] M. Kucher, M. Dannemann, R. Füßel, M.-T. Weber, N. Modler, Sliding friction and wear of human teeth against biocompatible polyether ether ketone (PEEK) under various wear conditions. Wear **486-487**, 204110 (2021). DOI: https://doi.org/10.1016/j.wear.2021.204110

[13] D. Kopp, C. Bandl, R. Kaindl, T. Prethaler, A.M. Coclite, W. Waldhauser, Shrouding gas plasma deposition technique for developing low-friction, wear-resistant WS2–Zn thin films on unfilled PEEK- The Relationship Between Process and Coating Properties. Coatings **14**, 1365 (2024). DOI: https://doi.org/10.3390/coatings14111365

[14] D. Kopp, M. Gleirscher, M. Stummer, L. Major, A. Hausberge, S. Schlogl, J.M. Lackner, R. Kaindl, T. Prethaler, A.M. Coclite, W. Waldhauser, Ternary low-friction coatings on thermoplastics by plasma spraying: Investigations on the process-structure. Surf. Coat. Technol. **477**, 130303 (2024). DOI: https://doi.org/10.1016/j.surfcoat.2023.130303

[15] R.J.K. Wood, Multifunctional Materials for Tribological Applications. First ed., Pan Stanford, Hoboken (2015).

[16] D. Kopp, J.M. Lackner, R. Kaindl, R. Elter, M. Stummer, A. Hinterer, A.M. Coclite, W. Waldhauser, Low-friction, wear-protecting coatings on polymers by atmospheric pressure plasma spraying. Surf. Coat. Technol. **448**, 128930 (2022). DOI: https://doi.org/10.1016/j.surfcoat.2022.128930

[17] T.W. Scharf, S.V. Prasad, Solid lubricants: a review. J. Mater. Sci. **48** (2), 511-531 (2013). DOI: https://doi.org/10.1007/s10853-012-7038-2

[18] B. Bhushan, Modern Tribology Handbook, first ed., CRC Press, Boca Raton (2000).

[19] F.P. Novais Antunesa, V.S. Vaissa, S.R. Tavaresa, R.B. Capazb, A.A. Leitão, Van der Waals interactions and the properties of graphite and 2H-, 3R- and 1T-MoS2: A comparative study. Comput. Mater. Sci. **152**, 146-150 (2018). DOI: https://doi.org/10.1016/j.commatsci.2018.05.045

[20] C. Richards, E. Jans, I. Gulko, K. Orr, I.V. Adamovich, N2 vibrational excitation in atmospheric pressure ns pulse and RF plasma jets. Plasma Sources Sci. Technol. **31**, 035010 (2022). DOI: https://doi.org/10.1088/1361-6595/ac6c1e

[21] G. Wulf, B. Mayer, U. Lommatzsch, Plasma co-polymerization of HMDSO and limonene with an atmospheric pressure plasma jet. Plasma **5**, 44-59 (2022). DOI: https://doi.org/10.3390/plasma5010004

[22] C. Corbella, S. Portal, M. Keidar, Flexible cold atmospheric plasma jet sources. Plasma **6**, 72-88 (2023). DOI: https://doi.org/10.3390/plasma6010007

[23] P. Harrison, L. Li, S. Wang, TEM study of FIB-lamellae from plasma-sprayed composite coatings on polymer substrates. Mater. Charact. **210**, 112789 (2024).

[24] M. Freschi, M. Di Virgilio, G. Zanardi, M. Mariani, N. Lecis, G. Dotelli, Employment of micro- and nano-WS2 structures to enhance the tribological properties of copper matrix composites. Lubricants **9**, 53 (2021). DOI: https://doi.org/10.3390/lubricants9050053

[25] Ł. Major, D. Kopp, B. Major, J.M. Lackner, Characterization of the Self-Dry-Lubrication and Self-Healing Effects on Nano- and Atomic Scale in Zn/MoS2/Graphite/Zn Coatings Deposited by Atmospheric Pressure Plasma Spraying on Ultra-Light Construction Polymers. Arch. Metall. Mater. **70**, 2, 905-911 (2025). DOI: https://doi.org/10.24425/amm.2025.153493

[26] L. Major, D. Kopp, B. Major, J.M. Lackner, Optimized APPJ-Deposited WS2/Zn Nanocoatings on PEEK: Insights into Nanoscale Wear Mechanisms, submitted to J. Mater. Res. Commun. (2025) (major revision).

[27] L. Chen, W. Wang, Q. Fang, K. Zuo, G. Hou, Q. Ai, Q. Li, L. Ci, J. Lou, High performance hierarchically nanostructured graphene oxide/covalent organic framework hybrid membranes for stable organic solvent nanofiltration. Appl. Mater. Today **20**, 100791 (2020). DOI: https://doi.org/10.1016/j.apmt.2020.100791

[28] S.S. Rawat, A.P. Harsha, O.P. Khatri, Tribological investigations of two-dimensional nanostructured lamellar materials as additives to castor-oil-derived lithium grease. J. Tribol. **144**, 091902 (2022). DOI: https://doi.org/10.1115/1.4054102